A&A 576, A47 (2015)
DOI: 10.1051/0004-6361/201424624

Astronomy & Astrophysics

Super-diffusion versus competitive advection: a simulation

D. Del Moro[1], F. Giannattasio[1], F. Berrilli[1], G. Consolini[2], F. Lepreti[3,4], and M. Gošić[5]

[1] Dipartimento di Fisica, Università degli Studi di Roma "Tor Vergata", via della Ricerca Scientifica 1, 00133 Roma, Italy
e-mail: delmoro@roma2.infn.it
[2] INAF–Istituto di Astrofisica e Planetologia Spaziali, via del Fosso del Cavaliere 10, 00133 Roma, Italy
[3] Dipartimento di Fisica, Università della Calabria, Ponte P. Bucci 31/C, 87036 Rende, Italy
[4] CNISM, Unità di Ricerca di Cosenza, Ponte P. Bucci 31/C, 87036 Rende, Italy
[5] Instituto de Astrofísica de Andalucía (CSIC), Apdo. 3004, 18080 Granada, Spain

Received 17 July 2014 / Accepted 22 January 2015

ABSTRACT

Context. Magnetic element tracking is often used to study the transport and diffusion of the magnetic field on the solar photosphere. From the analysis of the displacement spectrum of these tracers, it has recently been agreed that a regime of super-diffusivity dominates the solar surface. Quite habitually this result is discussed in the framework of fully developed turbulence.
Aims. However, the debate whether the super-diffusivity is generated by a turbulent dispersion process, by the advection due to the convective pattern, or even by another process is still open, as is the question of the amount of diffusivity at the scales relevant to the local dynamo process.
Methods. To understand how such peculiar diffusion in the solar atmosphere takes place, we compared the results from two different data sets (ground-based and space-borne) and developed a simulation of passive tracers advection by the deformation of a Voronoi network.
Results. The displacement spectra of the magnetic elements obtained by the data sets are consistent in retrieving a super-diffusive regime for the solar photosphere, but the simulation also shows a super-diffusive displacement spectrum: its competitive advection process can reproduce the signature of super-diffusion.
Conclusions. Therefore, it is not necessary to hypothesize a totally developed turbulence regime to explain the motion of the magnetic elements on the solar surface.

Key words. convection – hydrodynamics – turbulence – Sun: photosphere

1. Introduction

The outermost shell of the Sun is dominated by turbulent convection, which is the main driver of heat and entropy exchange between the different layers. The present analytical models of convective turbulence (namely, the mixing length theory and the full spectrum theory; Böhm-Vitense 1958; Canuto & Mazzitelli 1991; Canuto et al. 1996) are not able to describe appropriately the convective shell from the small subgranular scales ($\lesssim$100 km) to the global scale. On the other hand, the fully numerical aproaches (e.g. Beeck et al. 2012), while succesful in reproducing limited regions of the Sun, are also unable to provide a complete view because of the enormous range of temporal and spatial scales needed to simulate the whole solar convective envelope and the limited computing power available.

On the observational side, a viable way to study the convective flows on the solar surface are the small scale magnetic field elements since they are ubiquitous (Romano et al. 2012; Keys et al. 2014) and they (or their proxies, see Steiner et al. 2001; Uitenbroek & Tritschler 2006) are often used as tracers of the plasma flows (e.g. Bonet et al. 2008; Berrilli et al. 2013, 2014). Moreover, the study of the dynamics of the magnetic elements on the solar photosphere is of particular interest in astrophysics, since it could also provide constraints on

a) the characteristic spatiotemporal scales of the emergence and diffusion processes of the magnetic field (e.g. Orozco Suárez et al. 2012; Stangalini 2014);
b) the rates of interaction between the magnetic elements themselves, which can cause magnetic reconnections and subsequent micro-flaring events: a plausible mechanism for the heating of the upper solar atmosphere (as in the model of Viticchié et al. 2006).

In order to simplify the description of the motion of the magnetic elements, we neglect the force they exert on the surrounding plasma (Petrovay 1994, 2001), thus considering them as passive tracers of the underlying flows. This assumption has been verified in the quiet Sun (Viticchié et al. 2010; Orozco Suárez & Bellot Rubio 2012; Bellot Rubio & Orozco Suárez 2012; Giannattasio et al. 2013) where high values of β are observed.

In a Lagrangian approach, the trajectories of single magnetic elements are employed for a statistical determination of the dynamical properties of the ensemble. In particular, the magnetic element motion is described via the mean square displacement and modelled with a power law, $\langle\delta_r^2\rangle = k \cdot t^\gamma$, where $\langle\delta_r^2\rangle$ is the mean square displacement of the magnetic elements from their initial ($t = 0$) position, k plays the role of a diffusion coefficient, t is the time span from the magnetic element first detection, and γ is the so-called spectral index of the power law. For diffusive motions, if $\gamma = 1$, the diffusion is termed normal or Fickian (as in the case of the Random Walk scenario; Einstein 1905). When $\gamma \neq 1$ the diffusion is termed anomalous. Sub-diffusion if $\gamma < 1$ (the diffusion process is slower than normal diffusion); super-diffusion if $\gamma > 1$ (the process is more rapid than normal diffusion). It is worth noting that only in the case where $\gamma = 1$

does the constant k coincide with the diffusion coefficient. In the anomalous diffusion cases, the diffusion coefficient, defined as $k(\delta r, t) = \langle \delta_r^2 \rangle / t$, depends on the spatial and temporal scale (e.g. Schrijver et al. 1996; Chae et al. 2008; Abramenko et al. 2011; Lepreti et al. 2012).

The diffusion of magnetic elements has been studied by several authors through segmentation and tracking algorithms of photosperic data (see Goode et al. 2012, and references therein). The magnetic elements are detected using either the associated polarization (e.g. Viticchié et al. 2009) or their excess brightness in the G band (e.g. Sánchez Almeida et al. 2010); then, most authors utilize a Lagrangian approach to determine the spectral index γ (see e.g. Ruzmaikin et al. 1996; Utz et al. 2010; Kitiashvili et al. 2012). See for example Jafarzadeh et al. (2014) for the most recent review on the results obtained in previous works.

Apart from a few older reports (Schrijver & Martin 1990; Lawrence & Schrijver 1993; Cadavid et al. 1998, 1999), all the works on magnetic element diffusion agree on retrieving a super-diffusive behaviour (e.g. Wang & Sheeley 1993; Schrijver et al. 1996; Berger et al. 1998; Hagenaar et al. 1999; Chae et al. 2008; Abramenko et al. 2011; Chitta et al. 2012; Giannattasio et al. 2013, 2014a; Jafarzadeh et al. 2014) at all accessible spatio-temporal scales, ranging from granulation (diameter $\simeq$ 1 Mm and lifetime $\simeq$ few minutes; Muller 1999; Hirzberger et al. 1999; Del Moro 2004) to super-granulation (diameter $\simeq$ 30 Mm and lifetime $\simeq$ a day; Raju et al. 1999; Srikanth et al. 2000; Del Moro et al. 2004).

In the literature (e.g. Abramenko et al. 2011), $\langle \delta_r^2 \rangle$ is often called "average squared displacement" or "squared displacement spectrum" or simply "displacement spectrum". In the following, for the sake of clarity and to be consistent with previous literature we will use the term displacement spectrum when referring to the $\langle \delta_r^2 \rangle$ computed with magnetic element tracking.

In this work, we used an advection simulation to reproduce the scaling laws observed in the magnetic element motion on the solar photosphere. We assume that the plasma velocity structures (i.e. the granules) evolve under a simple mutual repulsion model, and that the dynamics on the granular scale is completely determined by the deformation of such granular structures. We consider the connected downflows on the solar photosphere as a sort of lattice-like network, and suppose the magnetic elements to be bonded to the photospheric velocity sinks located at the lattice junctions (the intergranular lane vertexes). Under such hypotheses, the simulation returns a super-diffusive regime with a scaling similar to that observed on the solar surface.

Therefore, a signal of super-diffusion can be imitated assuming that the magnetic elements are passively advected by the plasma downflow sinks and that the evolution of the granular pattern is a competitive expansion process.

2. Real data

In Figs. 1 and 2, we show the displacement spectrum $\langle \delta_r^2 \rangle$ for two different data sets imaging the quiet Sun. The plot in Fig. 1 was realized by computing the displacement of G-band bright points co-spatial with the magnetic field, as imaged by the ground-based instrument IBIS (Interferometric BIdimensional Spectropolarimeter; Cavallini et al. 2001; Cavallini 2006; Viticchié et al. 2009), located in the Dunn Solar Telescope of the National Solar Observatory (NM-USA). This analysis is similar to that in Abramenko et al. (2011), the main difference being the check of the magnetic origin of the G-band bright points allowed by the co-temporal magnetograms.

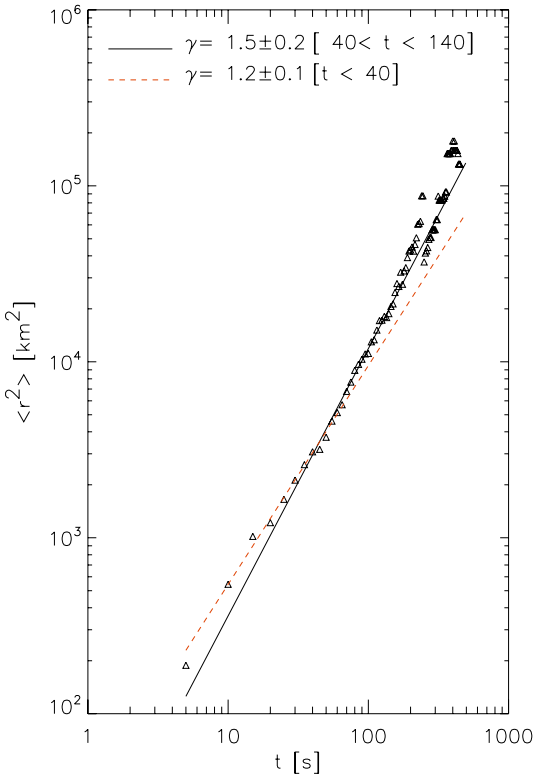

Fig. 1. Displacement spectrum for magnetic G-band bright points for a high-resolution data set acquired at the NSO-DST observatory. The lines represent power law fits for the ranges (t < 40 s) and (40 s $\leq t <$ 140 s).

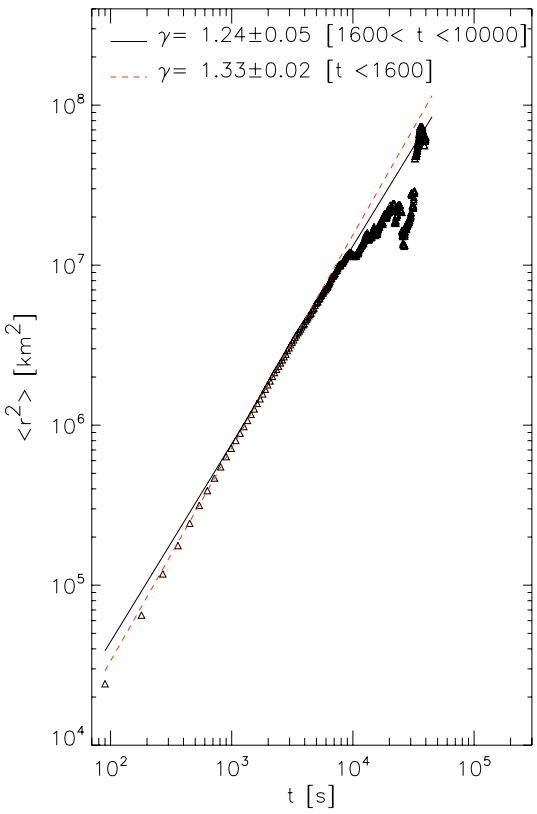

Fig. 2. Displacement spectrum for magnetic elements from a long-duration spectropolarimetric data set acquired by Hinode-NFI. The lines represent power law fits for the ranges (90 s $\leq t <$ 1600 s) and (1600 s $\leq t <$ 10 000 s).

Table 1. γ values retrieved by power law fits form the displacement spectra shown in Figs. 1 and 2 in different space and time ranges.

Space range [Mm]	Time range [s]	γ value
<0.05	<40	≃1.2
0.05−1.50	40−1600	≃1.4
>1.50	>1600	≃1.2

The spatial resolution of this data set, restored with multi-frame blind deconvolution (MFBD; Van Noort et al. 2006), is ≃0.″1, and the time between consecutive frames is dt = 5 s. The data have been $k_h - \omega$ filtered with a 7 km s^{-1} cut-off velocity. Since the data are affected by seeing, we tried to compensate this effect by applying a jitter removal algorithm. We subtracted a tip-tilt contribution from each bright point displacement. Such a contribution was estimated via the correlation of a 3.″3 × 3.″3 subframe centred on the bright point at two consecutive frames.

The plot in Fig. 2 was realized by computing the displacement of magnetic elements from the long-duration (∼25 h) data set acquired by Hinode-NFI (Kosugi et al. 2007; Tsuneta et al. 2008) and used in the analysis by Giannattasio et al. (2013, 2014a). The spatial resolution of this data set is ≃0.″3 and the time between consecutive frames is dt = 90 s; these data have also been $k_h - \omega$ filtered (for further details on the calibration see Gosic et al. 2012).

The tracking algorithm used for the two data sets is the same used in Giannattasio et al. (2013, 2014a) and presented in Del Moro (2004) and Berrilli et al. (2005). These two data sets combined allow us to explore more consistently the time range from 5 s to ≃10 000 s. They consistently identify a super-diffusive behaviour ($\gamma \simeq 1.4$) in the overlapping time range 90 s ≤ t < 500 s. We stress that, to our knowledge, this is the first time that two data sets acquired with rather different instruments and at different sites agree on retrieving γ values consistent within the errors.

3. Data interpretation

In the light of these two plots, whose results are summarized in Table 1, we put forward a possible interpretation.

For times shorter than 40 s (and hence for space scales smaller than ∼50 km), the displacement behaviour looks slightly super-diffusive: $\gamma \simeq 1.2$. Since that time scale is not explored by the Hinode data set, we cannot exclude a terrestrial atmosphere effect: despite the MFBD and the jitter correction, the G-band bright points may undergo deformations and displacements as a result of still uncorrected seeing aberrations. The seeing short (≪1 s) correlation times could affect the results. On the other hand, the G-band bright points are not perfect passive tracers: they have a structure of their own, which can be deformed by the surrounding plasma flows. Furthermore, buffeting-induced transverse oscillations like those found by Stangalini et al. (2013) could generate a signal likely to be detected as a movement of the tracer. These effects could mimic a random walk behaviour of the structure centre, for spatial scales ≲100 km. The third point we raise is that the short time range t < 40 s is lower than the correlation time scale of granulation, suggesting that, at least on short scales, $\gamma \simeq 1.2$ can really be the signature of anomalous diffusion by the intergranular turbulent flow field.

What happens for scales longer than ∼40 s and larger than ∼100 km? Why does γ increase and indicate a clear super-diffusive regime? At those spatial and time scales all the points raised above are no longer valid, and the magnetic elements behave like passive tracers on the large scale velocity field. Therefore, we interpret the $\gamma > 1$ regime as a real signal of super-diffusivity. Usually, this is explained as the result of a turbulent dispersion process and analysed in the framework of a fully developed turbulence. Instead, here we put forward the hypothesis that such an effect could be mainly due to the deformation of the lattice-like downflow network. Therefore, the displacement spectrum would also embed the contribution of the deformation of the network, which could be dominant at the large scales. To test this hypothesis, we developed a simplified computational model to simulate such a regime.

4. Simulation

To test our hypothesis and investigate the possible contribution of an advecting granular field in diffusing the tracers, we developed a simple simulation and studied the motion of the tracers embedded in.

Since the tracers used in the diffusion studies are often (if not always) embedded in the downflow network, we developed an algorithm mimicking the advective flow generated by a granular field similar to the solar photosphere. In this simulation, the tracers are the vertexes of a Voronoi tessellation generated from points representing the granule upflow centres. Such vertexes are simply advected by the flow generated by the evolution of the granules evolution, and no diffusive term is represented in the simulation. The interaction between the upflows of the granules is simulated by a repulsive force acting between the centres as a function of the associated upflow intensity. Stronger upflows tend to push away and squeeze weaker ones, causing an evolution of the Voronoi tessellation, which in this simulation represent the lattice-like downflow network. To take into account the granules that are pushed outside of the simulation box or are "squeezeed to death" by their neighbours (a sink term), we introduced a weak source term as the generation in a random position of new upflows to keep the number of granules constant. The motion of the tracers is therefore defined only by the deformation of the lattice-like pattern specified by the position of the upflows and their relative intensity.

The rules of the simulation are the following:

1) At t = 0, N = 1024 points are randomly distribuited on a 2048 × 2048 matrix, such that the average distance between them is 64 pixels.
2) Each point p has an associated interaction range $R(p)$ expressed in pixels. At t = 0, we initialize randomly $R(p)$ with a Gaussian distribution centred at 64 pixels and with a standard deviation of 6 pixels.
3) Every cycle, any point repels the other points within its $R(p)$ by 1 pixel.
4) At the end of the cycle, each point has its $R(p)$ decreased by the number of displacements it has undergone during the cycle due to the repulsion of the other points.
5) If a point is displaced out of the simulation bounds or its $R(p)$ falls below 1, it is replaced by another point in a random position and with $R(p) = 64 \pm 6$.
6) At the beginning of any cycle, all the $R(p)$ are incremented by a connectivity factor C = 4, to compensate for the displacements caused by 4 neighbours, on average.
7) The algorithm is iterated for 1000 cycles.

With the suitable choice of time step (dt = 15 s) and pixel scale (px = 1/64 arcsec), this algorithm simulates the interaction

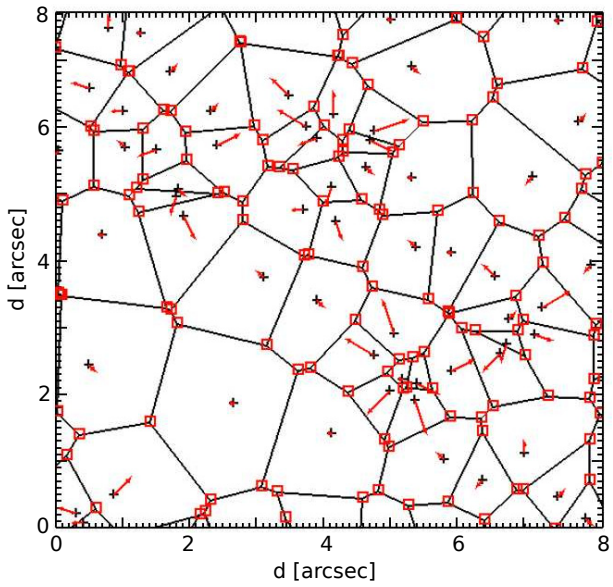

Fig. 3. A snapshot from the simulation. The black crosses represent the advection centres; the red vectors are the displacement (5× exaggeration) to be applied to the centres due to the neighbours' action; the red boxes on the Voronoi tesselation highlight the cell vertexes, which are used as tracers to compute the displacement spectrum. For the sake of visualization, only about a twentieth of the simulation domain is shown.

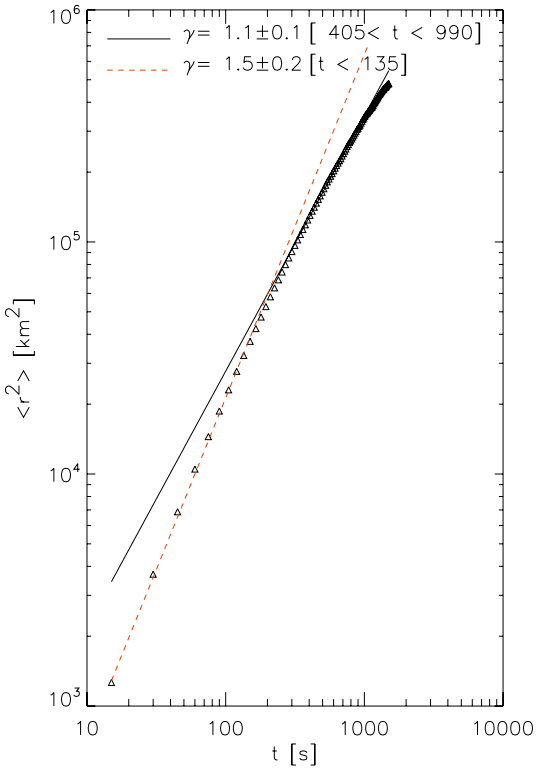

Fig. 4. Displacement spectrum for the Voronoi tessellation vertexes of the advection simulation. The lines represent power law fits for the ranges ($t < 135$ s) and (405 s $\leq t < 1000$ s).

between the upflows of the solar granulation. The granules in an underdense location will expand, growing a larger and larger $R(p)$, while granules in a more crowded location may shrink and disappear owing to (as a result of?) the other granules' pressure. After some iterations, the simulation reproduces a statistically steady, renovating granular pattern (a sample snapshot is shown in Fig. 3). We chose N, $R(p)_{t=0} = [64 \pm 6]$ and $C = 4$ to minimize this transient phase and to obtain an average granular size of ∼1 arcsec = 750 km on the solar surface. The choice of such values, corresponds to the assumption of that, on average, any granule interacts only with its closest [?] neighbours, since the average distance between centres is equal to the mean interaction range.

After the transient phase, on average, ∼15 granule centres have to be generated randomly in every cycle to compensate for those granules that moved out of the computation bounds or were suppressed. Thus, the simulation contains a weak sink/source term, since the loss or the injection of a granule centre changes the network pattern locally and cancels out/generates new Voronoi vertexes and therefore new tracers.

To be as consistent as possible with the real data analysis, we applied to the vertexes the same tracking algorithm used for the two data set in Figs. 1 and 2. We ran several simulations, using different parameter sets, obtaining consistently super-diffusive γ values, which are compatible with those retrieved by the observations (Giannattasio et al. 2013). The displacement spectrum retrieved by a sample simulation is shown in Fig. 4. The exponent retrieved by a power law fit for times shorter than 135 s is $\gamma \simeq 1.5$. For times longer than 400 s, the γ value decreases to $\simeq$1.1.

The transition point between the two behaviours has been estimated via a fitting procedure to be 200 ± 90 s. The errors on the γ values reported in the figure represent the variability of the fit results due to changes in the fitting ranges and not the fitting errors themselves, which are typically an order of magnitude smaller. Changing the time step dt or the pixel scale has no effect on the index γ. Changing instead the number of granules N, the connectivity C, or the shape of the distribution of $R(p)$ at $t = 0$, affects the average granule size and the duration of the transient phase. The γ values themselves depend weakly on the parameters N, $R(p)$, and C, which define the ratio between the average interaction range and the average granule dimension. The changes in the γ values due to small variations of the parameter sets are included in the reported errors. Instead, those parameters affect the position of the transition between the $\gamma \simeq 1.5$ and $\gamma \simeq 1.1$ regimes, since they set the spatio-temporal scale over which the flow can be considered isotropic: for a larger than average granule dimension and longer than the average granule duration.

5. Simulation discussion

The motion of the vertexes of a lattice-like pattern, undergoing deformation due to the mutual repulsion of the generating points, has a displacement spectrum with a spectral index $\gamma \simeq 1.5$. Given the parameters chosen for the simulation, the pattern produces a behaviour consistent with solar granulation: it shows cells that expand, collapse, and shuffle with characteristic time, velocity, and dimension close to the granular parameters. The displacement spectrum computed from the motion of the downflow vertexes of this simulation is totally defined by the pattern evolution, which has a single stochastic ingredient: the replacement of the removed upflows with new ones in random positions. Since we introduce only ∼10 new upflows on the $\sim 10^3$ existent upflows every step, we estimate this should be a small contribution. We recall that the number of new upflows introduced at

each iteration is a result of the Voronoi dynamics of the simulation (not a chosen parameter), which is determined by the set of the parameters discussed above. Therefore, the γ value obtained should derive only from the mutual interaction of the cells, which is neither entirely stochastic (which would lead to Brownian motion and $\gamma = 1$), nor ballistic ($\gamma = 2$).

6. Conclusions

Several works in the literature utilized a Lagrangian approach to determine the spectral index γ in the displacement spectra $\langle \delta_r^2 \rangle \sim t^\gamma$ of passive tracers on the solar photosphere (e.g. Ruzmaikin et al. 1996; Utz et al. 2010; Abramenko et al. 2011; Kitiashvili et al. 2012). The most recent among these works (see Jafarzadeh et al. 2014, and references therein), agree in retrieving a $\gamma > 1$ value, suggesting that a super-diffusion regime is present in the solar photosphere.

In this paper, we computed with the same algorithm the displacement spectra of magnetic elements from two spectropolarimetric data sets: one from a ground-based instrument (IBIS at NSO/DST) and the other from a space-borne instrument (NFI on-board Hinode satellite). We confirm the super-diffusive motion of these elements, but put forward an alternative interpretation in terms of the deformation of the lattice-like structure advecting the tracers, instead of the fully developed turbulence framework used so far.

To substantiate this interpretation, we realized a simple simulation of an advection process mimicking the granular flows on the solar surface and used the vertexes of the simulated granular cell as tracers. In this simulation, the motion of the tracers is entirely determined by the deformation of the lattice-like downflow network modelling the solar surface flow patterns. When analysed with the same approach as the real data sets, the simulation showed a displacement spectrum with a super-diffusive ($\gamma \simeq 1.5$) behaviour.

This result confirms that other theoretical frameworks may be used to interpret the motion of the magnetic elements on the solar surface, and that the diffusion parameters calculated from the displacement spectrum analysis may not necessarily be related to the effects of a turbulent regime.

For example, Escande & Sattin (2007) investigated theoretically some cases when the $\boldsymbol{v}$ term in the advection-diffusion equation cannot be cancelled by changing the reference frame (the Lagrangian approach): in the hypothesis of an evolving advection field, the tracers can jump from one cell to another and enter into long flights, depending on the characteristic temporal, spatial, and intensity scales of the advection field. This point of view is definitely not far from the simple simulation we put forward.

In parallel, Solomon et al. (1994) explored experimentally different regimes, from quasi-periodic to chaotic and to turbulent regimes, finding that both the quasi-periodic and the chaotic regimes are characterized by Lévy flights and show super-diffusion with $\gamma \simeq 1.5$.

Other analogies between the views of Escande & Sattin (2007) and Solomon et al. (1994) and our algorithm and the possibility of further extending their results (by applying the pair separation approach of Giannattasio et al. 2014b), are at the moment under investigation.

Acknowledgements. This work is partially supported by a Ph.D. grant at University of Rome Tor Vergata and by the Italian MIUR-PRIN grant 2012P2HRCR on "The active Sun and its effects on Space and Earth climate" and by the Space Weather Italian COmmunity (SWICO) Research Program. Financial support by the Spanish Ministerio de Economía y Competitividad through project AYA2012-39636-C06-05 (including a percentage from European FEDER funds) is gratefully acknowledged. Part of the data used in this work were acquired in the framework of Hinode Operation Plan 151, entitled "Flux replacement in the solar network and internetwork". Hinode is a Japanese mission developed and launched by ISAS/JAXA, collaborating with NAOJ as a domestic partner, NASA and STFC (UK) as international partners. Scientific operation of the Hinode mission is conducted by the Hinode science team organized at ISAS/JAXA. This team mainly consists of scientists from institutes in the partner countries. Support for the post-launch operation is provided by JAXA and NAOJ (Japan), STFC (UK), NASA, ESA, and NSC (Norway). Part of the data used in this work were acquired with IBIS at NSO/DST under the proposal ID T748. NSO is operated by the Association of Universities for Research in Astronomy (AURA), Inc. under cooperative agreement with the National Science Foundation.

References

Abramenko, V. I., Carbone, V., Yurchyshyn, V., et al. 2011, ApJ, 743, 133
Beeck, B., Collet, R., Steffen, M., et al. 2012, A&A, 539, A121
Bellot Rubio, L. R., & Orozco Suárez, D. 2012, ApJ, 757, 19
Berger, T. E., Loefdahl, M. G., Shine, R. S., & Title, A. M. 1998, ApJ, 506, 439
Berrilli, F., Del Moro, D., Russo, S., Consolini, G., & Straus, T. 2005, ApJ, 632, 677
Berrilli, F., Scardigli, S., & Giordano, S. 2013, Sol. Phys., 282, 379
Berrilli, F., Scardigli, S., & Del Moro, D. 2014, A&A, 568, A102
Böhm-Vitense, E. 1958, Z. Astrophys., 46, 108
Bonet, J. A., Márquez, I., Sánchez Almeida, J., Cabello, I., & Domingo, V. 2008, ApJ, 687, L131
Cadavid, A. C., Lawrence, J. K., Ruzmaikin, A. A., Walton, S. R., & Tarbell, T. 1998, ApJ, 509, 918
Cadavid, A. C., Lawrence, J. K., & Ruzmaikin, A. A. 1999, ApJ, 521, 844
Canuto, V. M., & Mazzitelli, I. 1991, ApJ, 370, 295
Canuto, V. M., Goldman, I., & Mazzitelli, I. 1996, ApJ, 473, 550
Cavallini, F. 2006, Sol. Phys., 236, 415
Cavallini, F., Berrilli, F., Cantarano, S., & Egidi, A. 2001, Mem. Soc. Astron. It., 72, 554
Chae, J., Litvinenko, Y. E., & Sakurai, T. 2008, ApJ, 683, 1153
Chitta, L. P., van Ballegooijen, A. A., Rouppe van der Voort, L. R., DeLuca, E. E., & Kariyappa, R. 2012, ApJ, 752, 48
Del Moro, D. 2004, A&A, 428, 1007
Del Moro, D., Berrilli, F., Duvall, T. L., Jr., & Kosovichev, A. G. 2004, Sol. Phys., 221, 23
Einstein, A. 1905, Annalen der Physik, 322, 549
Escande, D. F., & Sattin, F. 2007, Phys. Rev. Lett., 99, 185005
Giannattasio, F., Del Moro, D., Berrilli, F., et al. 2013, ApJ, 770, L36
Giannattasio, F., Stangalini, M., Berrilli, F., Del Moro, D., & Bellot Rubio, L. 2014a, ApJ, 788, 137
Giannattasio, F., Berrilli, F., Biferale, L., et al. 2014b, A&A, 569, A121
Goode, P. R., Abramenko, V., & Yurchyshyn, V. 2012, Phys. Scr., 86, 018402
Gosic, M., Katsukawa, Y., Bellot Rubio, L., & Orozco Suarez, D. 2012, 39th COSPAR Scientific Assembly, 39, 657
Jafarzadeh, S., Cameron, R. H., Solanki, S. K., et al. 2013, A&A, 563, A101
Hagenaar, H. J., Schrijver, C. J., Title, A. M., & Shine, R. A. 1999, ApJ, 511, 932
Hirzberger, J., Bonet, J. A., Vázquez, M., & Hanslmeier, A. 1999, ApJ, 515, 441
Keys, P. H., Mathioudakis, M., Jess, D. B., Mackay, D. H., & Keenan, F. P. 2014, A&A, 566, A99
Kitiashvili, I. N., Abramenko, V. I., Goode, P. R., et al. 2012, Physica Scripta, submitted [arXiv:1206.5300]
Kosugi, T., Matsuzaki, K., Sakao, T., et al. 2007, Sol. Phys., 243, 3
Lawrence, J. K., & Schrijver, C. J. 1993, ApJ, 411, 402
Lepreti, F., Carbone, V., Abramenko, V. I., et al. 2012, ApJ, 759, L17
Majda, A. J., & Kramer, P. R. 1999, Phys. Rep., 314, 237
Muller, R. 1999, Motions in the Solar Atmosphere, 239, 35
Orozco Suárez, D., & Bellot Rubio, L. R. 2012, ApJ, 751, 2
Orozco Suárez, D., Katsukawa, Y., & Bellot Rubio, L. R. 2012, ApJ, 758, L38
Petrovay, K. 1994, Solar Surface Magnetism, Proc. NATO Advanced Research Workshop, held Soesterberg, the Netherlands, November 1–5, 1993, eds. R. J. Rutten, & C. J. Schrijver (Dordrecht: Kluwer Academic Publishers), 415

Petrovay, K. 2001, Space Sci. Rev., 95, 9
Raju, K. P., Srikanth, R., & Singh, J. 1999, Bull. Astron. Soc. India, 27, 65
Romano, P., Berrilli, F., Criscuoli, S., et al. 2012, Sol. Phys., 280, 407
Ruzmaikin, A. A., Cadavid, A. C., Chapman, G. A., Lawrence, J. K., & Walton, S. R. 1996, ApJ, 471, 1022
Sánchez Almeida, J., Bonet, J. A., Viticchié, B., & Del Moro, D. 2010, ApJ, 715, L26
Schrijver, C. J., & Martin, S. F. 1990, Sol. Phys., 129, 95
Schrijver, C. J., Shine, R. A., Hagenaar, H. J., et al. 1996, ApJ, 468, 921
Solomon, T. H., Weeks, E. R., & Swinney, H. L. 1994, Physica D Nonlinear Phenomena, 76, 70
Srikanth, R., Singh, J., & Raju, K. P. 2000, ApJ, 534, 1008
Stangalini, M. 2014, A&A, 561, L6
Stangalini, M., Solanki, S. K., Cameron, R., & Martínez Pillet, V. 2013, A&A, 554, A115
Steiner, O., Hauschildt, P. H., & Bruls, J. 2001, A&A, 372, L13
Tsuneta, S., Ichimoto, K., Katsukawa, Y., et al. 2008, Sol. Phys., 249, 167
Uitenbroek, H., & Tritschler, A. 2006, ApJ, 639, 525
Utz, D., Hanslmeier, A., Muller, R., et al. 2010, A&A, 511, A39
Van Noort, M., Rouppe van der Voort, L., & Lofdahl, M. 2006, ASP Conf. Ser., 354, 55
Viticchié, B., Del Moro, D., & Berrilli, F. 2006, ApJ, 652, 1734
Viticchié, B., Del Moro, D., Berrilli, F., Bellot Rubio, L., & Tritschler, A. 2009, ApJ, 700, L145
Viticchié, B., Del Moro, D., Criscuoli, S., & Berrilli, F. 2010, ApJ, 723, 787
Wang, Y.-M., & Sheeley, Jr., N. R. 1993, ApJ, 414, 916